Optimization under Uncertainty for Efficient Laser Powder Bed Fusion Manufacturing

Yulin Guo and Boris Kramer

Department of Mechanical and Aerospace Engineering, University of California San Diego

East Coast Optimization Meeting 2025 | April 17, 2025

Laser powder bed fusion

UC San Diego

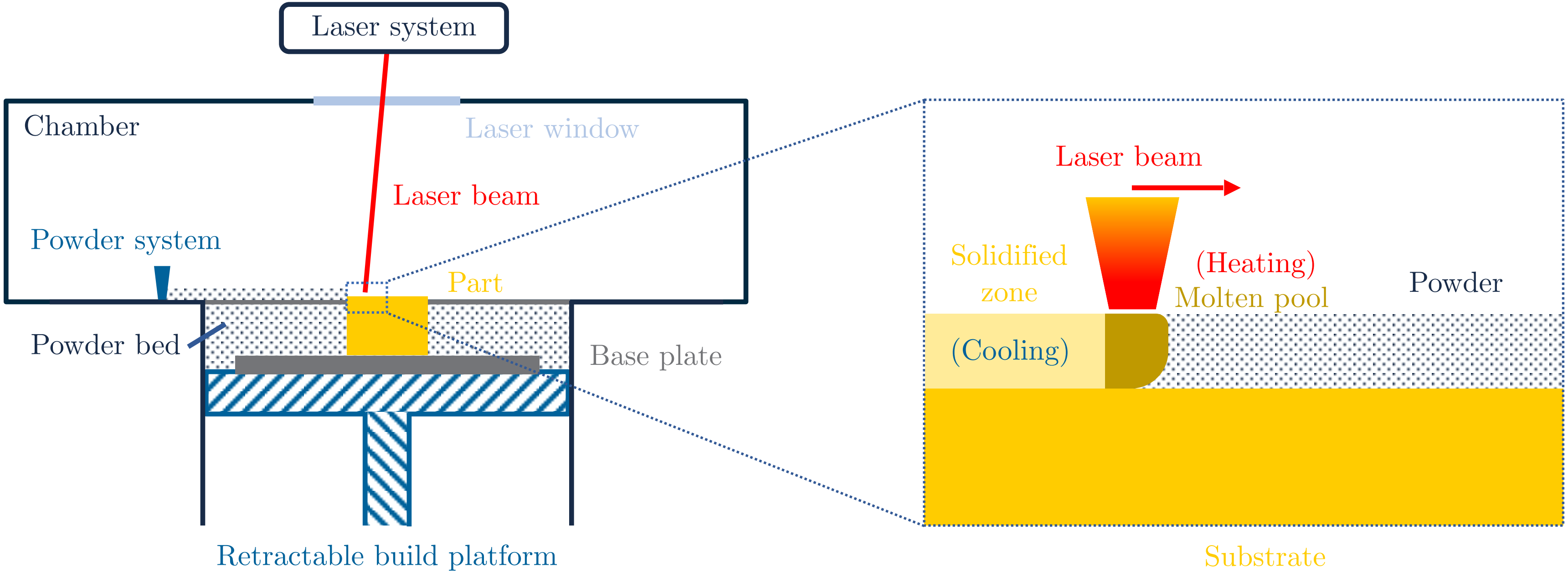

- **Goal: part qualification** ~ process parameters (laser power, scanning speed, etc.)

Problem overview

UC San Diego

$$
\begin{aligned}
\min_{P,v} \quad & Pl/v \\
\text{subject to} \quad & \bar{p}_t(\sigma_{\max}(P, v, \boldsymbol{Z}; \boldsymbol{\theta})) \leq 1 - \alpha_T, \\
& T_{\text{liq}} < T_{\max} < 1.1 \times T_{\text{liq}}, \\
& P_L \leq P \leq P_U, \\
& v_L \leq v \leq v_U
\end{aligned}
$$

Energy consumption

Buffered probability of failure constraint on stress

Constraint on liquidus temperature

Bounds on laser power

Bounds on scanning speed

- Design variables: laser power P, scanning speed v
- Simulate printing process in Abaqus with weakly-coupled thermal and mechanical models
  - Gaussian-form heat flux from laser
  - Elastic-plastic strain and thermal strain

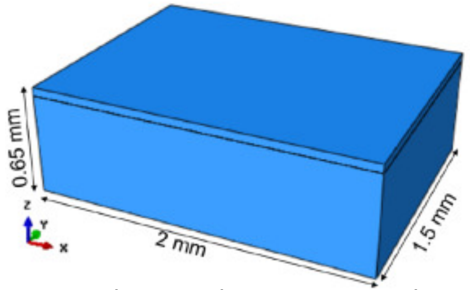

One simulation: about 0.75 CPU hours

Buffered probability of failure $\bar{p}_t$

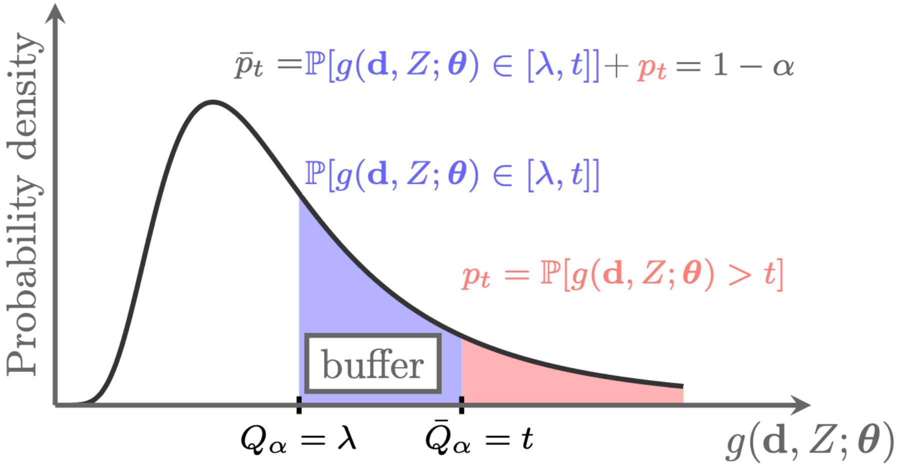

- Adds a buffer to probability of failure
- Considers the magnitude of failure in addition to failure frequency
- Eliminates the guess work associated with choosing safety margins

Surrogate models

$P, v, \boldsymbol{Z}; \boldsymbol{\theta}$ → Thermal model → Temperature field $\boldsymbol{T}$ → Mechanical model → Stress field $\boldsymbol{\sigma}$

Surrogate models

$P, v, \boldsymbol{Z}; \boldsymbol{\theta} \rightarrow$ **Thermal model** $\rightarrow$ Temperature field $\boldsymbol{T}$ $\rightarrow$ **Mechanical model** $\rightarrow$ Stress field $\boldsymbol{\sigma}$

Data from
N simulations

31 time instances

$\mathbf{T} \in \mathbb{R}^{N \times 31}$

Max von Mises stress

$\mathbf{S} \in \mathbb{R}^{N \times 448}$

Surrogate models

$P, v, \boldsymbol{Z}; \boldsymbol{\theta}$ → **Thermal model** → Temperature field $\boldsymbol{T}$ → **Mechanical model** → Stress field $\boldsymbol{\sigma}$

Data from
N simulations

$\Big\downarrow$ SVD

Features

31 time instances

$\mathbf{T} \in \mathbb{R}^{N \times 31}$

$\mathcal{T}_{:,1}, \mathcal{T}_{:,2}, \ldots, \mathcal{T}_{:,31}$

Max von Mises stress

$\mathbf{S} \in \mathbb{R}^{N \times 448}$

$\mathcal{S}_{:,1}, \mathcal{S}_{:,2}, \ldots, \mathcal{S}_{:,448}$

Surrogate models

$P, v, \boldsymbol{Z}; \boldsymbol{\theta}$ → Thermal model → Temperature field $\boldsymbol{T}$ → Mechanical model → Stress field $\boldsymbol{\sigma}$

Active subspace discovery

	Temperature	Stress
Data from N simulations	31 time instances $\mathbf{T} \in \mathbb{R}^{N \times 31}$	Max von Mises stress $\mathbf{S} \in \mathbb{R}^{N \times 448}$
↓ SVD		
Features	$\mathcal{T}_{:,1}, \mathcal{T}_{:,2}, \ldots, \mathcal{T}_{:,31}$	$\mathcal{S}_{:,1}, \mathcal{S}_{:,2}, \ldots, \mathcal{S}_{:,448}$
↓		
Active variables	$\boldsymbol{\eta}_{\mathbf{T}}$	$\boldsymbol{\eta}_{\mathbf{S}}$

Surrogate models

$P, v, \boldsymbol{Z}; \boldsymbol{\theta}$ → **Thermal model** → Temperature field $\boldsymbol{T}$ → **Mechanical model** → Stress field $\boldsymbol{\sigma}$

Active subspace discovery

	Temperature	Stress
Data from N simulations	31 time instances $\mathbf{T} \in \mathbb{R}^{N \times 31}$	Max von Mises stress $\mathbf{S} \in \mathbb{R}^{N \times 448}$
↓ SVD Features	$\mathcal{T}_{:,1}, \mathcal{T}_{:,2}, \ldots, \mathcal{T}_{:,31}$	$\mathcal{S}_{:,1}, \mathcal{S}_{:,2}, \ldots, \mathcal{S}_{:,448}$
Active variables	$\boldsymbol{\eta}_{\mathbf{T}}$	$\boldsymbol{\eta}_{\mathbf{S}}$
Surrogate models	$\hat{G}_{\mathcal{T}_{:,j}}(\boldsymbol{\eta}_{(j_{\boldsymbol{T}})}) \approx \mathcal{T}_{:,j}((P, v, z; \boldsymbol{\theta}))$	$\hat{G}_{\mathcal{S}_{:,j}}(\boldsymbol{\eta}_{(j_{\boldsymbol{S}})}) \approx \mathcal{S}_{:,j}((P, v, z; \boldsymbol{\theta}))$

Surrogate models

$P, v, \boldsymbol{Z}; \boldsymbol{\theta}$ → **Thermal model** → Temperature field $\boldsymbol{T}$ → **Mechanical model** → Stress field $\boldsymbol{\sigma}$

Active subspace discovery

Data from N simulations	31 time instances	Max von Mises stress
	$\mathbf{T} \in \mathbb{R}^{N \times 31}$	$\mathbf{S} \in \mathbb{R}^{N \times 448}$
↓ SVD		
Features	$\mathcal{T}_{:,1}, \mathcal{T}_{:,2}, \ldots, \mathcal{T}_{:,31}$	$\mathcal{S}_{:,1}, \mathcal{S}_{:,2}, \ldots, \mathcal{S}_{:,448}$
Active variables	$\boldsymbol{\eta}_{\mathbf{T}}$	$\boldsymbol{\eta}_{\mathbf{S}}$
Surrogate models	$\hat{G}_{\mathcal{T}_{:,j}}(\boldsymbol{\eta}_{(j_{\boldsymbol{T}})}) \approx \mathcal{T}_{:,j}((P, v, z; \boldsymbol{\theta}))$	$\hat{G}_{\mathcal{S}_{:,j}}(\boldsymbol{\eta}_{(j_{\boldsymbol{S}})}) \approx \mathcal{S}_{:,j}((P, v, z; \boldsymbol{\theta}))$
Approximations	$\hat{\mathbf{T}}$	$\hat{\mathbf{S}}$

Choosing the number of features

UC San Diego

$$\mathrm{err}_{\mathbf{T}}(k) = \frac{1}{120}\sum_{i=1}^{120}\frac{\|\mathbf{T}_{i,:} - \hat{\mathbf{T}}_{i,:}(k)\|_2}{\|\mathbf{T}_{i,:}\|_2}$$

$$\mathrm{err}_{\mathbf{S}}(k) = \frac{1}{120}\sum_{i=1}^{120}\frac{\|\mathbf{S}_{i,:} - \hat{\mathbf{S}}_{i,:}(k)\|_2}{\|\mathbf{S}_{i,:}\|_2}$$

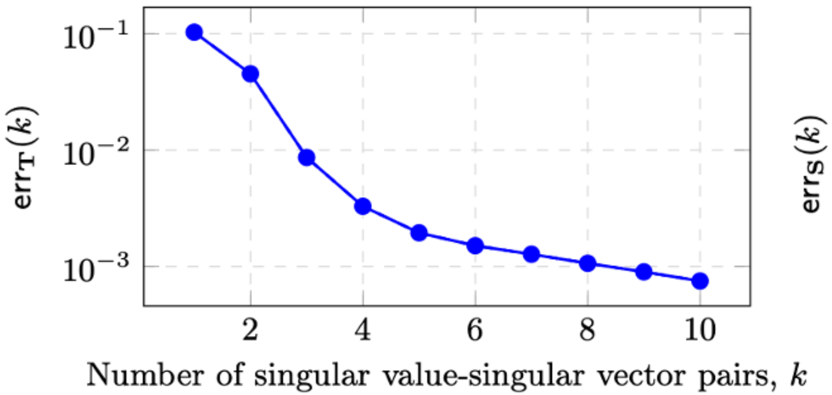

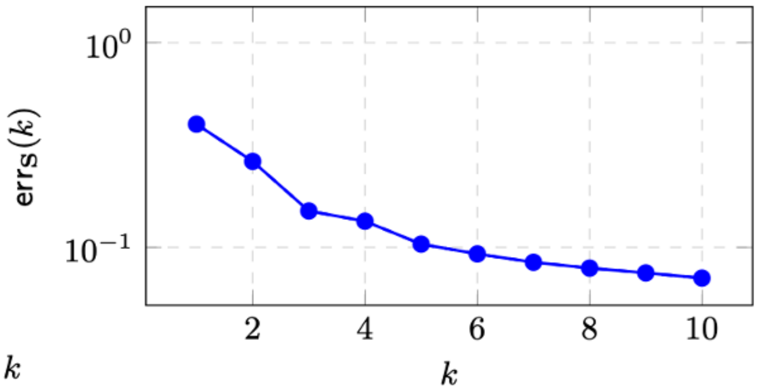

Number of features $K_{\mathcal{T}}^{*} = 2$ $K_{\mathcal{S}}^{*} = 6$

Surrogate model: feature vs active variable

Thermal model – feature 1

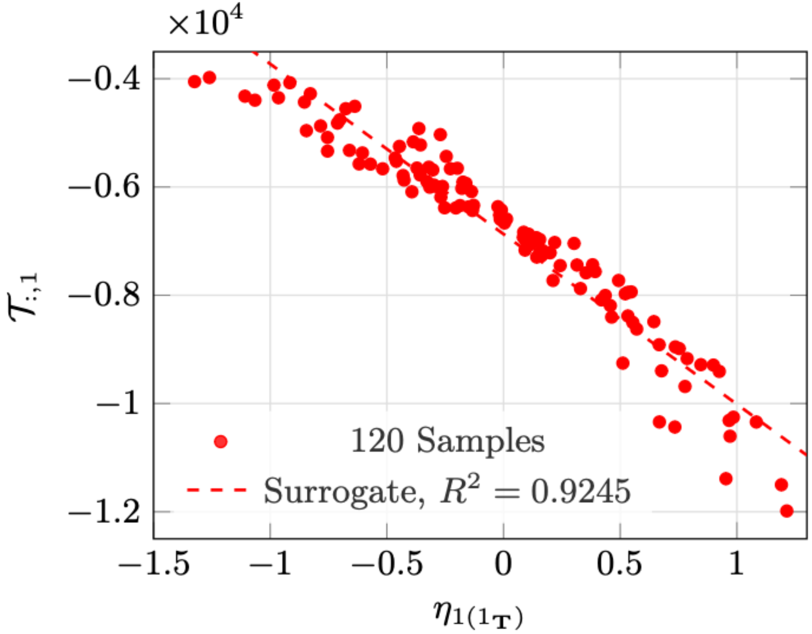

Mechanical model – feature 1

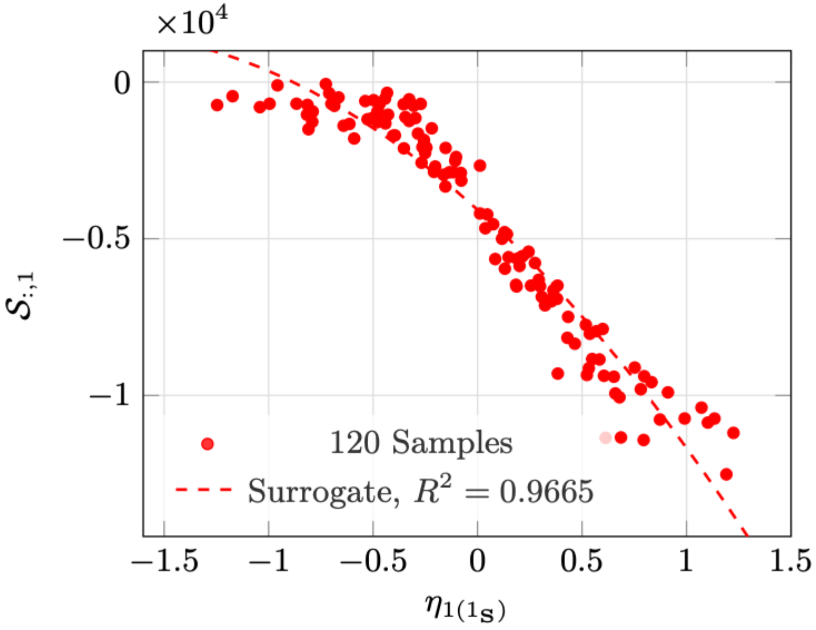

Optimization results

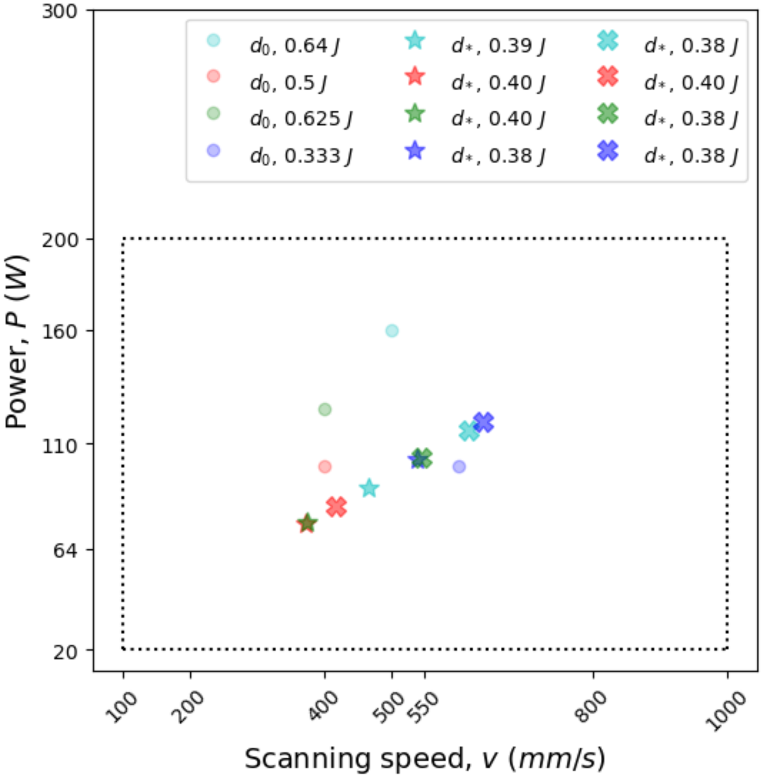

- Optimizations with 4 different initial guesses
- SLSQP and COBYLA solvers
- All converged to consumed energy of about 0.4J

Optimization results

UC San Diego

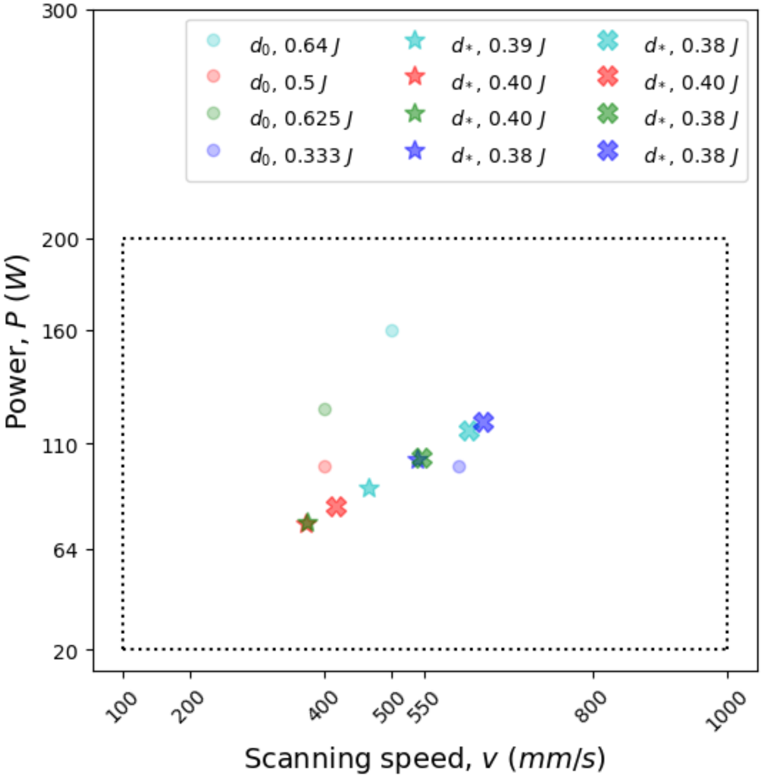

- Optimizations with 4 different initial guesses
- SLSQP and COBYLA solvers
- All converged to consumed energy of about 0.4J

Validation

- [417.33 mm/s, 82.97 W], $\bar{Q}_{0.95}$ = 762.08 MPa
- 50 FEM simulations, $\bar{Q}_{0.95}$ = 768.12 MPa

-0.79%

Optimization results

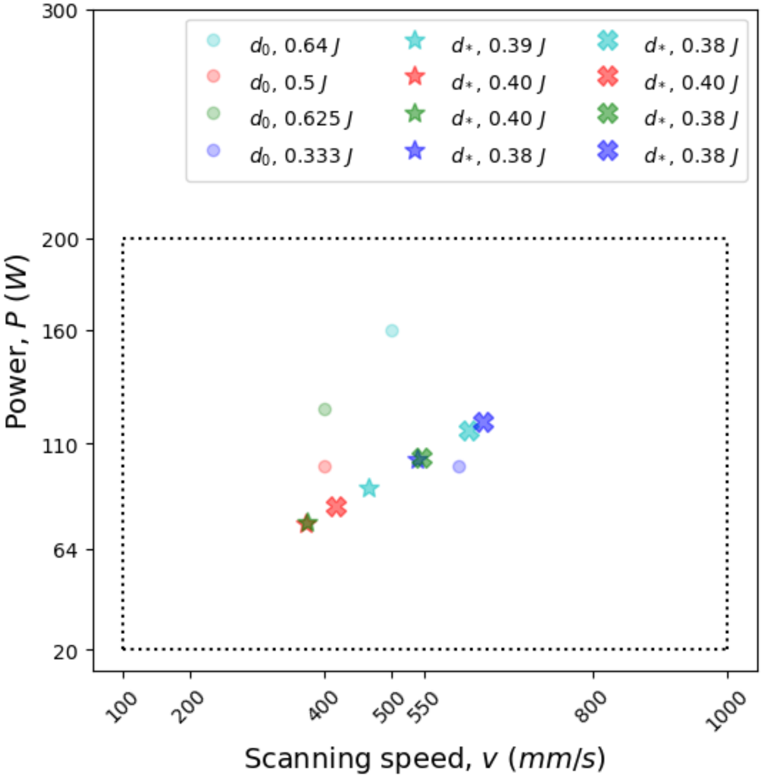

- Optimizations with 4 different initial guesses
- SLSQP and COBYLA solvers
- All converged to consumed energy of about 0.4J

Validation

- [417.33 mm/s, 82.97 W], $\bar{Q}_{0.95}$ = 762.08 MPa
- 50 FEM simulations, $\bar{Q}_{0.95}$ = 768.12 MPa

-0.79%

- [614.5 mm/s, 115.8 W], $\bar{Q}_{0.95}$ = 790.69 MPa
- 50 FEM simulations, $\bar{Q}_{0.95}$ = 804.89 MPa

-1.76%

Conclusion

- BPOF-constrained design optimization enhances manufacturing quality while minimizing energy
- Finite element analysis captures the thermal and mechanical behavior of the manufactured part
- Surrogate models for temperature and residual stress via SVD and active subspace discovery to reduce computational costs while maintaining prediction accuracy
- Validated optimization through independent FEA: decreased energy and reduced build failures

Funding: Air Force Office of Scientific Research (PM Fahroo) under award number FA9550-24-1-0237

yulinguo.com